Energy Conversion and Management 300 (2024) 117978

Contents lists available at ScienceDirect

Energy Conversion and Management

journal homepage: www.elsevier.com/locate/enconman

Comparative study of high-solid anaerobic digestion at laboratory and industrial scale – Process performance and microbial community structure

Ebba Perman [a,b], Maria Westerholm [a,b], Tong Liu [a,c], Anna Schnürer [a,b,*]

[a] Department of Molecular Sciences, Swedish University of Agricultural Sciences, Uppsala, Sweden
[b] Biogas Solutions Research Center, Linköping, Sweden
[c] Department of Forest Ecology and Management, Swedish University of Agricultural Sciences, Umeå, Sweden

ARTICLE INFO

Keywords:
High-solid anaerobic digestion
Laboratory-scale plug-flow reactor
Process performance
Microbial community structure

ABSTRACT

High-solid anaerobic digestion (HSD) for biogas production, compared with wet digestion, is attracting interest due to advantages such as reduced fresh water usage, improved digestate quality and potential for high organic loading rates. However, the underlying processes are not well described and evaluated for HSD. In this study, two laboratory-scale reactors (46 L) of plug-flow type were designed to simulate an industrial-scale HSD process co-digesting food waste, agricultural waste and garden residues under thermophilic conditions. Performance of the laboratory-scale HSD process under stable and disturbed conditions was compared with that in industrial-scale reactors. The results showed that the laboratory- and industrial-scale processes had similar efficiency (93 %) and VS-reduction (43 % and 41 %, respectively) and relatively similar specific methane production (339 and 366 NL CH_4/kg VS, respectively). Results from tracer studies combined with chemical analyses showed no phase-separation or plug-flow behaviour along the horizontal axis in either laboratory- or industrial-scale reactors, indicating a need for further process optimisation. Analyses of microbial community structure showed high similarity between laboratory- and industrial-scale, but with some differences caused by downscaling. During the experiment, the laboratory- and industrial-scale processes both showed signs of disturbance, *i.e.* VFA accumulation at NH_4^+-N levels > 4 g/L, accompanied by a shift in microbial community structure at both scales, with significant increases in relative abundance of *e.g.* genera *Defluviitoga* and *Methanothermobacter*. In conclusion, this study confirmed the validity of simulating HSD at laboratory scale, thus providing valuable insights into biogas production from high-solid substrates, both in laboratory- and industrial-scale processes.

1. Introduction

Anaerobic digestion (AD) is a process in which organic materials are degraded and converted into biogas, a renewable energy source [1,2]. The residual material from the process, *i.e.* the digestate, has a high content of plant-available nutrients and can be used as biofertiliser [3,4]. Industrial-scale AD is widely used for treatment of organic waste streams, *e.g.* sewage sludge, agricultural residues and food waste from households and industries [5]. The most commonly applied AD technology is wet digestion, where the total solids (TS) content is < 15 % [6]. This technology is well-investigated and established at industrial scale. An alternative, less commonly applied technology is high-solid digestion (HSD), which typically operates with TS > 15 % [6]. HSD has several advantages over wet AD, such as lower use of fresh water for substrate dilution and the potential to use relatively high organic loading rate (OLR), and thus smaller reactor volumes in relation to input substrate [7]. Another advantage compared with wet digestion is that the digestate produced has a lower water content and higher nutrient concentration [7]. The dry nature of many agricultural wastes, *e.g.* crop residues and animal solid manure, and of food waste make these substrates suitable for digestion in HSD processes [8]. However, more research is needed to achieve high reliability and profitability at industrial scale [6,9].

Irrespective of the technology used for AD, the substrate is degraded

Abbreviations: AD, anaerobic digestion; VFA, volatile fatty acids; CSTR, continuous stirred-tank reactor; PFR, plug-flow reactor; HSD, high-solid digestion; TS, total solids; VS, volatile solids; OLR, organic loading rate; HRT, hydraulic retention time; SMP, specific methane production; RMP, residual methane production; SAOB, syntrophic acetate-oxidising bacteria.

* Corresponding author at: Department of Molecular Sciences, Swedish University of Agricultural Sciences, Box 7015, Uppsala SE-750 07, Sweden.
E-mail address: anna.schnurer@slu.se (A. Schnürer).

https://doi.org/10.1016/j.enconman.2023.117978
Received 19 September 2023; Received in revised form 14 November 2023; Accepted 6 December 2023
Available online 15 December 2023

by a diverse community of anaerobic microorganisms in four main steps: i) hydrolysis of polymers to monomers, ii) fermentation of monomers to volatile fatty acids (VFAs) and alcohols, iii) anaerobic oxidation of fermentation products to the main methanogenic substrates acetate and H_2/CO_2 and iv) methanogenesis [1]. Conversion of VFAs is strictly dependent on a close syntrophic relationship between bacteria performing anaerobic oxidation and methanogens [1,10]. For an efficient process, all AD steps need to be synchronised. When there is a kinetics imbalance between acid production and consumption rates, VFA accumulation can occur [11].

HSD processes are generally operated at relatively high OLR [8,9,12]. Thus the risk of process disturbances and VFA accumulation is high compared with wet AD, particularly for easily degradable substrates with high protein content, such as food waste [13–16]. During degradation of proteins, ammonium-nitrogen (NH_4^+-N) is released and at high concentrations this can cause inhibition of the microbial community, especially methanogens, resulting in problems with acid conversion [17,18]. Co-digestion with more recalcitrant carbon-rich materials, *e.g.* plant materials, paper or solid manure with high levels of lignocellulose, has been observed to improve process stability [12,14,16,19–21].

In addition to the above-mentioned biological obstacles, HSD also involves some technical challenges relating to use of materials with high TS content, including issues with mixing highly viscous materials with large particle size. To tackle these issues, continuous HSD processes are often run using plug-flow reactors (PFR) [9,22], rather than the continuous stirred tank reactors (CSTR) commonly applied for wet digestion. Horizontal PFRs are fed from one end and digestate is taken out from the other end, and inside the reactor the material is pushed from the feeding inlet to the digestate outlet. In an ideal system there is no horizontal mixing or diffusion, which would create separate reaction zones along the length of the reactor, like a series of CSTRs but within the same reactor [23–25]. Operation at close-to-ideal plug-flow conditions could thereby theoretically give a process similar to multi-phase anaerobic digestion set-up, with phase separation between the hydrolysis/acidification steps at the start of the reactor and methanogenesis towards the end [9,25–27]. Modelling evaluations have suggested that minimal diffusion along the reactor can optimise process efficiency [28], although this could also be problematic in cases of local accumulation of inhibitors [29]. In the ideal case, material resides in the reactor during exactly one hydraulic retention time (HRT) [24], which eliminates short-circuiting of readily accessible organic compounds and thereby optimises substrate utilisation. However, to the best of our knowledge, only one study has previously validated plug-flow behaviour in a lab-scale AD reactor of horizontal PFR type [30]. Thus, the necessary conditions for establishing phase-separated plug-flow in terms of substrate characteristics, process operation and technology remain unclear, which highlights the importance of more investigations on PFRs. Moreover, the microbiology of PFRs and whether distinct separation of the biological steps can be achieved has been investigated in only a few previous studies [31,32].

To maximise efficiency, resource utilisation and economic performance, AD processes must be operated under optimised conditions. New optimisation strategies are best explored using laboratory-scale reactors, thereby avoiding decreases in productivity and risks of process failure in large-scale reactors during the experiments. However, this means that processes at laboratory and industrial scale must be comparable and that the laboratory results can be scaled up. Promising results in this regard were obtained by Gallert *et al.* [33], who optimised OLR at laboratory scale and successfully applied the results in a full-scale AD process. Moreover, Bouallagui *et al.* [34] found laboratory-scale evaluation to be useful for prediction of performance in a full-scale reactor treating sewage sludge and Lüdtke *et al.* [35] observed good agreement in methane production from an industrial-scale process mimicked at laboratory scale. However, these studies were all carried out in CSTR systems and when it comes to HSD systems of plug-flow type there is a lack of comparative studies at laboratory and industrial scale. Moreover, few previous studies have studied the effect of upscaling or downscaling on microbial community structure and links to process performance.

The main aim of this study was thus to investigate whether HSD processes can be operated in the laboratory with the same efficiency and yield as in an industrial-scale system, and thereby serve as a useful model for evaluation of process operation. An additional aim was to investigate plug-flow behaviour and phase separation in laboratory- and industrial-scale reactors. A thermophilic industrial-scale HSD process fed a mixture of food waste, agricultural residues and garden waste was mimicked in the laboratory. The laboratory-scale and industrial-scale reactors were both horizontal PFRs, with three sampling ports along the reactor. Process performance and plug-flow or phase separation between reactor sections were evaluated using chemical and microbiological methods and the processes were assessed under both stable and disturbed conditions.

2. Methods

2.1. High-solid laboratory- and industrial-scale reactors

High-solid digestion of mixed organic waste (see below) was evaluated at laboratory scale for 53 weeks and at industrial scale for 44 weeks. Duplicate laboratory-scale reactors (LR1, LR2) of plug-flow type with horizontal orientation were designed in-house, each with an active volume of 45.7 L (filled to 85 % of reactor height) and a length:width (L:W) ratio of 4.1 (Fig. 1). The industrial-scale system consisted of triplicate reactors of plug-flow type (RK1, RK2, RK3), each with an active volume of 2,100 m^3 (filled to 85 % of reactor height) and L:W ratio of 5.3.

The laboratory-scale reactors were stirred radially at a speed of 1 rpm by six paddle blades scraping the inside walls. Material was added through a feeding funnel and digestate was removed from the other end of the reactor (Fig. 1). The reactors had three sections (S1, S2, S3), each with a separate sampling point, and reactor material flowed freely between the sections. The industrial-scale reactors were constructed similarly, with three sections and radial stirrers (~0.5 rpm), although with slightly higher L:W ratio and different feeding inlets, using a screw instead of a funnel. Due to practical difficulties, section S2 in the industrial-scale reactors was only sampled on one occasion (microbiological analysis in week 33). Sampling was carried out weekly from S1 and S3 of both the laboratory- and industrial-scale reactors.

Digestate from the industrial-scale reactors was used as inoculum for the laboratory-scale process. Before inoculation, the digestate was sieved to reduce the particle size to 15 mm and contaminating waste (plastics etc.) was removed. The industrial scale reactors were operated under thermophilic conditions (53–56 °C) to achieve hygienisation during the digestion process and similar conditions were used also in laboratory scale (52–53 °C). Temperature sensors were placed at three positions along all reactors (Fig. 1). At both scales, digestate (without any post-treatment) was recirculated at an average ratio of 30 % of ingoing substrate mass. Recirculation in laboratory scale was carried out manually at each feeding occasion by mixing parts of the discharged digestate with the substrate fed to the feeding inlet. Volumetric HRT was ~ 42 days in laboratory-scale reactors, and HRT and OLR were calculated based on substrate input, excluding the recirculated material. To avoid volume reduction in the laboratory-scale reactors due to gas production, reduction of volatile solids (VS) was estimated to 50 % and was compensated for daily by adjusting the recirculation ratio. The laboratory-scale reactors were fed semi-continuously once per day, six days per week. The industrial-scale reactors were fed semi-continuously for 12 h per day, seven days per week, and the average volumetric HRT was ~ 33 days.

2.2. Substrate characteristics

The substrate consisted of different organic waste fractions: food waste, garden residues, horse manure, olive cake, crop residues (wheat)

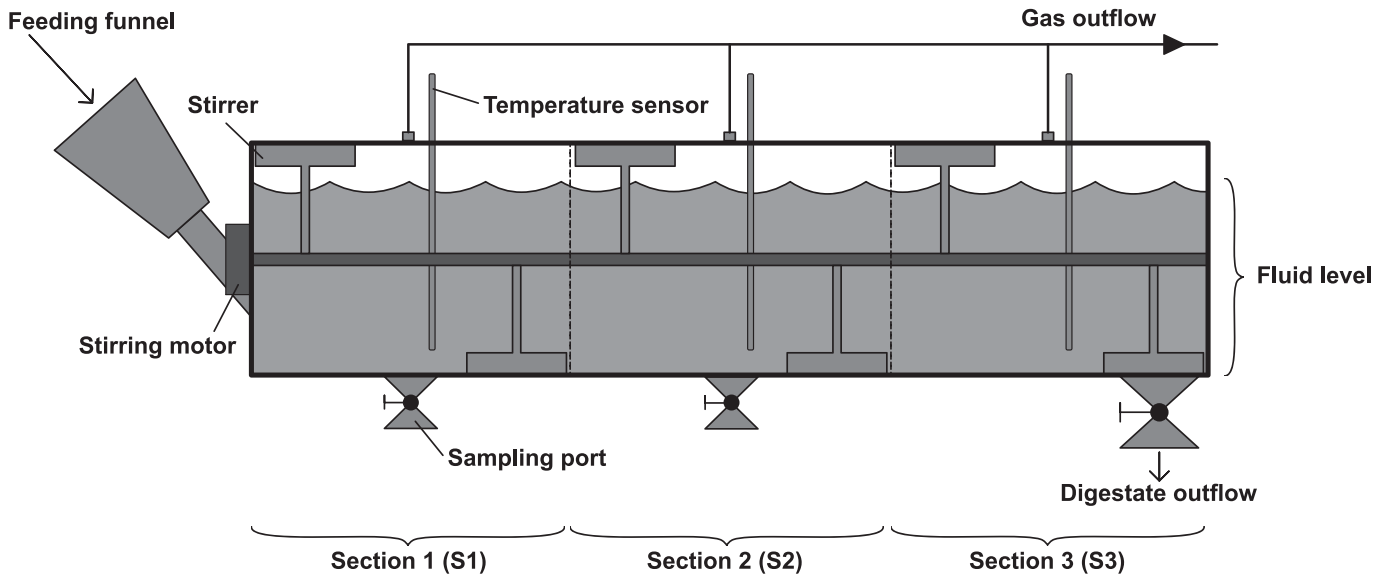

Fig. 1. Schematic illustration of the laboratory-scale high-solid reactor used in the presentstudy.

and potato waste (Table A.1). At industrial scale the substrate was shredded and sieved to particle size ~ 60 mm before being fed into the reactors, with an average VS_{in} of 23 %. Due to variations in the substrate supply chain at the plant, the ratios of different substrate fractions differed somewhat from day to day. Therefore, it was not feasible to collect homogenous substrate samples representing the entire mixture from the industrial-scale reactors. Instead the different substrate fractions were collected sperately and later mixed for use in laboratory scale.

The substrate used in laboratory-scale was mixed to mimick the ratios used in the industrial process (based on the average substrate composition during 24 weeks before the start of the experiment). The substrate fractions were collected at the industrial-scale plant to use the same substrate in both scales. For practical reasons, substrate fractions used in laboratory scale were collected every 3–4 months during the experimental period and stored at 4 °C until use. At laboratory scale, the substrates were pre-treated by grinding to particle size ~ 10 mm. All fractions were analysed for TS and VS, and the final substrate mixes were analysed for total N and C, organic N, NH_4^+-N, and concentration of macromolecules (Table 1). Before feeding the reactors, water was added to the substrate mix to obtain a final VS_{in} of 22 %.

2.3. Analytical methods

The volume of gas produced in the laboratory-scale reactors was measured continuously using RITTER Drum-type meters TG0.5 (RITTER Apparatebau GmbH & Co. KG, Bochum, Germany). Gas composition (CH_4, CO_2, O_2, H_2, H_2S) was measured before every feeding occasion, using an AwiFLEX device (Awite Bioenergie Gmbh, Langenbach).

Concentrations of TS and VS in substrate fractions and digestate samples were analysed in triplicate using standard methods (APHA, 1998). Potential VFA losses during TS analyses were investigated (based on SGC Rapport 2013:273) but found to be negligible, and thus no correction was made for VFA losses.

Table 1
Chemical composition of substrate mixes used in laboratory-scale reactors during different periods of operation.

Substrate period	Week 1–14	Week 14–25	Week 26–53
Tot-N [g/kg]	5.1	6.8	5.1
Org-N [g/kg]	4.7	6.1	5.0
NH_4^+-N [g/kg]	0.4	0.7	0.1
Tot-C [g/kg]	108.5	122.3	90.2
Raw protein [g/kg]	ND	33.4	26.8
Raw fat [g/kg]	ND	35.7	19.6
Carbohydrates [g/kg]	ND	155.7	146.1

ND, not determined.

Organic N (SS-ISO 13 878), NH_4^+-N (FOSS TECATOR, Application Note, AN 5226, based on ISO 11732) and total C (SS-ISO 10 694) in substrate samples were measured by Agrilab AB (Uppsala, Sweden). Biweekly measurements of NH_4^+-N concentration in digestate samples from the laboratory-scale reactors were performed using a LCK 302 Ammonium kit (Hach Lange Gmbh, Düsseldorf, Germany). In brief, digestate samples were sieved using a tea-strainer and then frozen at −20 °C until analysis. Before analysis, samples were thawed and centrifuged at 11500xg for 15 min. The supernatant was removed and diluted in dH_2O, sterile filtered (0.2 μm syringe filter), and then finally added to the test cuvette (200 μL), following the manufacturer's instructions. Absorbance was measured using a DR3900 spectrophotometer (Hach, Germany). Ammonia-nitrogen (NH_3-N) concentration was calculated based on temperature, pH and NH_4^+-N concentration [36].

The concentration of VFA in digestate samples from laboratory-scale reactors was measured by HPLC (Agilent 1100 Series, Agilent Technologies, Waldbronn, Germany), as described previously [37]. Digestate samples were sieved using a tea-strainer and then frozen at −20 °C until sample preparation and analysis. Alkalinity and the ratio between volatile organic acids and total inorganic carbon (FOS/TAC) was measured on fresh, sieved (using tea-strainer) digestate samples from laboratory reactors by titration with 0.1 N H_2SO_4 Standard Solution, using a TitraLab AT1000 Series (Hach Lange Gmbh) according to the manufacturer's instructions, based on the Nordmann method for FOS/TAC measurement.

The protein content in digestate and substrate samples was calculated based on total Kjeldahl-N (EN 13342) and NH_4^+-N (STANDARD METHODS 1998, 4500 mod.) measured by Eurofins Food & Feed Testing Sweden (Lidköping). Carbohydrate content (SLVFS 1993:21) was analysed by Eurofins Environment Testing Sweden AB, and content of raw fat (NMKL 160 mod.) by Eurofins Food & Feed Testing Sweden (Lidköping).

For digestate samples from the industrial-scale reactors, the following analyses were performed: TS (SS-EN 12880:2000), VS (SS-EN 12879:2000), VFA (Clarus 550 gas chromatograph (Perkin Elmer, Waltham, MA, USA) with a packed Elite-FFAP column (Perkin Elmer, USA) for acidic compounds (Jonsson & Borén, 2002)), pH (SS-EN ISO 10523:2012) and NH_4^+-N (ISO 5664:1984). All these analyses were

carried out by Tekniska verken i Linköping AB (Linköping, Sweden).

2.4. Tracer test

Plug-flow behaviour was evaluated in laboratory-scale reactor LR1 with a tracer test using LiCl (Alfa Aesar, ThermoFisher (Kandel) GmbH, Germany), with an average concentration in the reactor of 91 mg Li^+/kg TS [38]. Digestate for recirculation was collected before the tracer was added and was used for recirculation throughout the test. Samples of outgoing digestate were taken on every feeding occasion (6 days/week) for a period of 40 days. Digestate was analysed for Li^+ concentration (SS 028150:1993/SS-EN, ISO 11885:2009) by Eurofins Environment Testing Sweden AB. A tracer test using Li^+ had been performed at the industrial-scale plant, to ensure sufficient residence time for hygienisation. In that test, $LiOH{\cdot}H_2O$ (Helm AG, Hamburg, Germany) was added to one of the reactors to obtain an average Li^+ concentration of 25 mg/kg TS and the Li^+ concentration in the outgoing digestate was measured regularly during the first 48 h. During the test, the reactor was operated under minimum HRT conditions (~25 days), *i.e.* fed the maximum possible substrate amount to simulate a "worst-case scenario". It was estimated that the amount of outgoing digestate during the test was 0.5–0.75 m^3/hour. Analysis of Li^+ concentration in digestate samples was carried out by Agrolab GmbH, Germany.

2.5. Analyses of microbial community

Microbial community structure was analysed by 16S rRNA gene sequencing on two occasions. First, samples from steady-state operation were analysed to compare the different reactor sections (S1-S3) and laboratory- and industrial-scale reactors. Samples at laboratory scale were collected during the start-up phase (before week 1) and in experiment weeks 11 and 14, from all three reactor sections of LR1 and LR2. Samples from S1 and S3 in industrial-scale reactors RK2 and RK3 (RK1 excluded due to process disturbance) were collected in experiment weeks 6, 13, 20, 28 and 33. During week 33, a sample was also taken from S2 in RK3. In the second sequencing round, samples from the period with process disturbances, as observed by VFA accumulation, were collected (18 time points for the two laboratory-scale reactors and 12 time points for the three industrial-scale reactors). DNA extraction was performed as a single replicate (for samples in time-series with ≥ 3 sampling time-points) or three replicates per time-point, using the FastDNA Spin Kit for Soil (MP Biomedicals Europe) as described previously [39]. All samples were stored at −20 °C, both before and after DNA extraction.

Libraries of the 16S rRNA gene were prepared using primers for amplification of the V4 region (515′F/806R). Library preparation and sequencing (Illumina Novaseq platform) was carried out by Novogene (UK) Company Limited, Cambridge, United Kingdom. Raw sequences (with primer and barcode sequences removed) were processed using the DADA2 pipeline v1.16.0 [40]. Optimal trimming sites to minimise error rates were chosen using the tool Figaro [41]. Sequences were annotated with the Silva database v138.1 [42]. Processing of results was carried out in R, using the phyloseq package v1.38.0. Weighted principal coordinate analysis (PCoA) was used to analyse β-diversity in different reactors and sections at steady state. Distances were calculated by the UniFrac method [43] based on a phylogenetic tree generated using neighbour-joining [44], using the phangorn package in R.

The gene copy number of archaeal groups in samples from the steady-state period was investigated by qPCR targeting the 16S rRNA gene. Two different primer pairs were used, designed for detection of orders Methanobacteriales (MBT) and Methanomicrobiales (MMB) [45]. The qPCR protocol and programme were as described previously [37]. Before analysis, sample dilution was tested [46] and the optimal dilution was found to be 100x. The qPCR reaction was run with a QuantStudio 5 Real-Time PCR system (ThermoFisher Scientific), and the raw data were processed using QuantStudio Design & Analysis Software v1.5.2 (ThermoFisher Scientific).

2.6. Degradation efficiency and residual methane production

Residual methane potential (RMP) and degradation rate of protein (egg white powder, Källbergs Industri AB, Töreboda, Sweden), cellulose (microcrystalline cellulose, Alfa Aesar, ThermoFisher GmbH, Kandel, Germany) and fat (rapeseed oil) were measured in digestate samples, taken from both S1 and S3, from laboratory (pooled digestate from LR1 and LR2) and industrial-scale (RK3) , in principle as described previously [47]. Batch tests for analysis of degradation rates were carried out in triplicate with 200 mL digestate and 2 g VS/L of added substrate in bottles with total volume 600 mL. RMP *i.e.,* background methane production, was measured in digestate without substrate addition. Methane production were measured during 28 days incubation at 52 °C in AMPTS II systems (Bioprocess Control, Lund, Sweden).

Volatile solids reduction was calculated as $(VS_{in}\text{-}VS_{out})/VS_{in}$ [32].

Based on RMP, methane production per active reactor volume (MP_V) and HRT, process efficiency (%) was calculated according to Rico *et al.* [48] as: Efficiency (%) $= 100*(MP_V*HRT)/(MP_V*HRT + RMP)$.

2.7. Statistical analyses

The process parameters VFA concentration, VS content, VS reduction, pH, specific methane production (SMP), RMP, NH_3-N, and NH_4^+-N concentration were compared between the laboratory-scale and industrial-scale reactors, and also between sections S1 and S3 within each reactor. Sections were compared using paired *t*-test, within reactor and at the same time point. For comparisons between laboratory- and industrial-scale reactors, values from S3 in both systems were compared using Welch's *t*-test assuming unequal variances. All statistical analyses were carried out in R v4.1.2.

3. Results

3.1. Process parameters and performance in the laboratory- and industrial-scale systems

At laboratory scale, mean SMP was 338 ± 57 and 339 ± 47 NL CH_4/kg VS in LR1 and LR2, respectively (Table 2), with no significant difference between the two replicate reactors. Weekly average SMP varied constantly in the laboratory-scale process, but no general descending or

Table 2
Overview of the laboratory-scale and industrial-scale processes, based on measurements on digestate samples taken from the last section (S3) of the reactors. Mean values or minimum–maximum range during the experiment is shown where appropriate.

Parameter	Laboratory-scale	Industrial-scale
OLR [g VS/L day]	5.2[a]	4.2–8.4
$VS_{substrate}$ [%]	22[b]	19–25
TS_{out} [%]	13.6–22.8	15.1–23.9
VS_{out} [%]	10.8–14.2	10.6–16.4
HRT [days]	~42	~33
Recirculation rate [% of ingoing material, ww]	30	30
Weekly average SMP [NL CH_4/kg VS]	200–563 (LR1) 183–464 (LR2)	269–466
Total VFA [g/L]	0.1–9.0	0.2–12.9
NH_4-N (NH_3-N) [g/L]	2.1–4.6 (0.7–2.0)	2.3–4.1 (0.3–1.7)
pH	8.0–8.5	7.5–8.7
Alkalinity [mg $CaCO_3$/L]	14 261–24 284	ND[c]
RMP[d] [NmL CH_4/g inoculum]	5.2 ± 0.4	5.9 ± 0.5

[a] OLR during stable process.
[b] All substrate batches diluted to 22% VS content on ww basis.
[c] Not determined.
[d] Mean value and standard deviation over nine replicates.

increasing trend over time was observed (Fig. 2a). In industrial-scale reactors, SMP was calculated based on the total amount of gas produced in all three reactors per week (Fig. 2b). The mean value over the whole experiment period was 366 ± 52 NL CH_4/kg VS (Table 2).

The OLR was kept constant when the laboratory-scale processes were stable, but had to be lowered to 75 %, 50 % or even 0 % during process disturbance events (Fig. B.1). The process was considered stable when daily volumetric gas production was relatively constant from day-to-day and when there was no significant increase in CO_2 and H_2 content in the gas (Fig. B.1). The FOS/TAC-value was also considered an indicator of process stability, and OLR was decreased when a steep increase in this parameter was observed (Fig. B.1). Changes in process performance, indicating process disturbance, were observed in laboratory-scale reactors around experiment weeks 20–45 in LR1 and 25–35 in LR2. These changes included increasing NH_4^+-N and VFA concentrations, with propionate concentration reaching 6.2 and 4.2 g/L in LR1 and LR2,

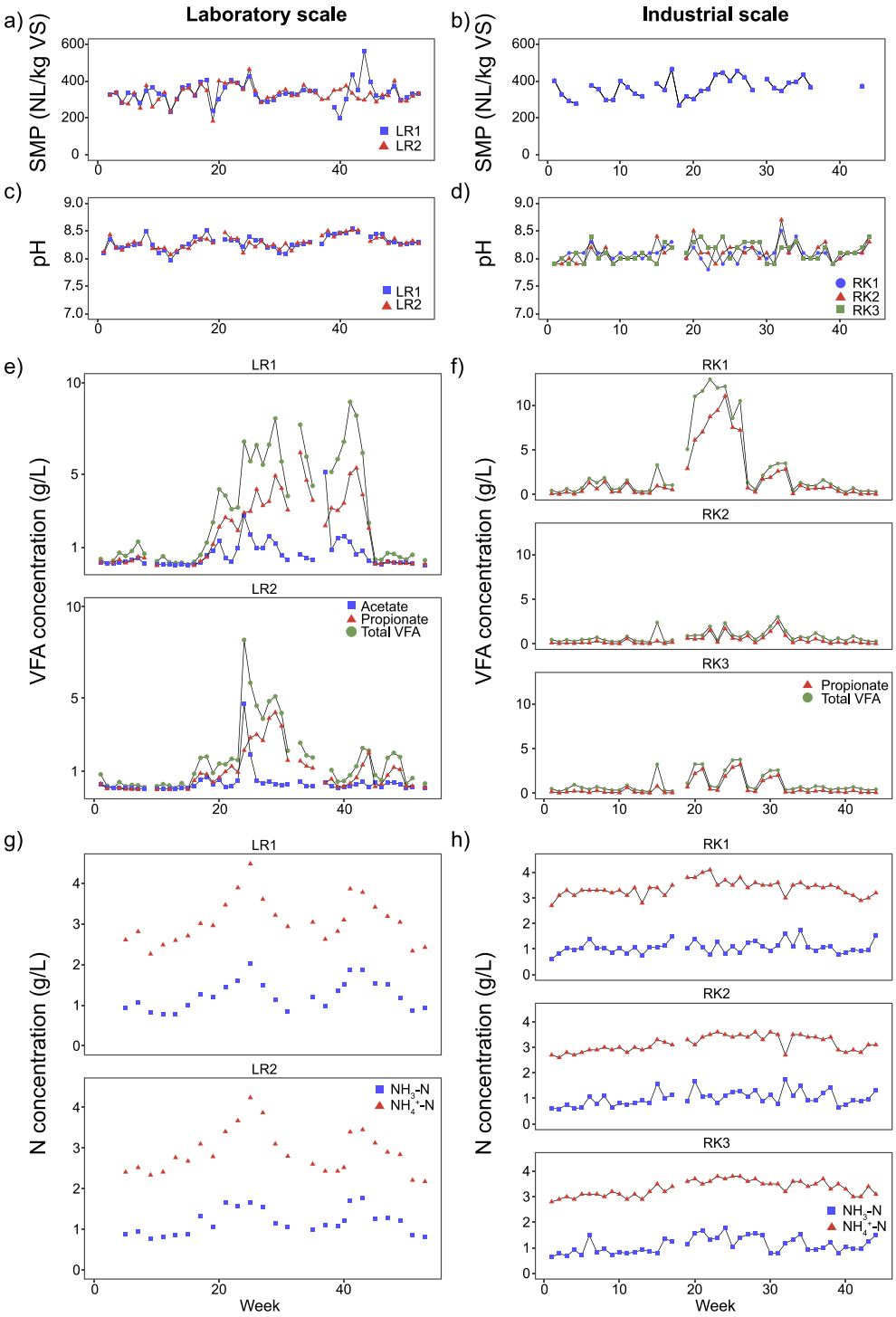

Fig. 2. Process data from (left) laboratory-scale reactors (LR1, LR2) and (right) industrial-scale reactors (RK1, RK2, RK3). Specific methane production at a) laboratory and b) industrial scale (mean production from all three reactors). pH in outgoing digestate (S3) at c) laboratory and d) industrial scale. e) Total VFA, acetate and propionate concentration at laboratory scale and f) total VFA and propionate concentration at industrial scale, all measured in outgoing digestate (S3). Concentration of NH_3-N and NH_4^+-N in outgoing digestate (S3) at g) laboratory and h) industrial scale.

respectively (Fig. 2e, Fig. B.2). Additionally, H_2S and CO_2 content in the gas increased, a sharp peak in H_2 was observed and the CH_4 content dropped slightly (Fig. B.1). However, pH remained relatively stable throughout the entire experimental period (Fig. 2c).

In the industrial-scale reactors, the variation in OLR depended on substrate availability and no adjustments were made based on process performance. During the experimental period, the OLR ranged between 4.2 and 8.4 g VS/L day, with a mean value of 6.9 g VS/L day (Fig. B.1 and Table 2). Process parameters such as pH, NH_4^+-N concentration and gas composition remained relatively stable throughout the experimental period (Fig. 2d, 2 h, Table 2 and Fig. B.1). However, RK1 showed a disturbance during experiment weeks 19–26, with a peak in VFA concentration, mainly represented by propionate reaching 11.0 g/L (Fig. 2f). In reactors RK2 and RK3, the VFA concentration fluctuated during the same weeks but did not reach the same level as in RK1. During the same period, a peak in NH_4^+-N concentration was observed, reaching the highest values in RK1 (Fig. 2h).

3.2. Comparison of process parameters and performance between systems and sections

Comparison of process performance between laboratory and industrial scale revealed several significant differences, with higher VFA concentrations and pH at laboratory scale and higher NH_4^+-N concentrations and VS_{out} at industrial scale (Fig. 3a-d, Table C.1). Mean SMP and RMP were also higher at industrial compared with laboratory scale (Fig. 3f-g). On average, NH_4^+-N levels were higher in industrial-scale reactors, but the relatively high pH in laboratory-scale reactors led to significantly higher levels of free ammonia at laboratory (0.8–2.0 g NH_3-N/L) than industrial scale (0.6–1.8 g NH_3-N/L) ($p = 0.006$).

Comparisons of process parameters were also made between reactor sections S1 and S3 in all reactors, at both laboratory and industrial scale (Fig. 3a-d, 3f, Table C.1). In the laboratory-scale reactors, significant differences between sections were seen in VFA concentration and alkalinity, but not in VS content, pH, NH_4^+-N concentration or RMP. In the industrial-scale reactors, there were significant differences between reactor sections in VFA concentration, pH, NH_4^+-N concentration, VS content and RMP.

To study plug-flow behaviour, a tracer study was carried out using Li^+. At laboratory scale, around 60 % of total Li^+ added to the reactor left the system within 40 days (Fig. D.1). The highest Li^+ concentration in outflowing digestate was seen after 3–4 days (Fig. D.2). A tracer test was also carried out at the industrial-scale plant, for 48 h in total to ensure sufficient residence time for hygienisation. The Li^+ concentration in outgoing digestate from the industrial-scale reactors exceeded the background level ~ 19 h after addition of tracer, but the majority of added Li^+ was not detected during the test period (data not shown).

3.3. Substrate degradation, degradation rates and macromolecule concentrations

VS reduction was measured to evaluate the extent of organic fraction degraded in the reactors. Although VS reduction varied more between time points in the industrial-scale system, the average value was

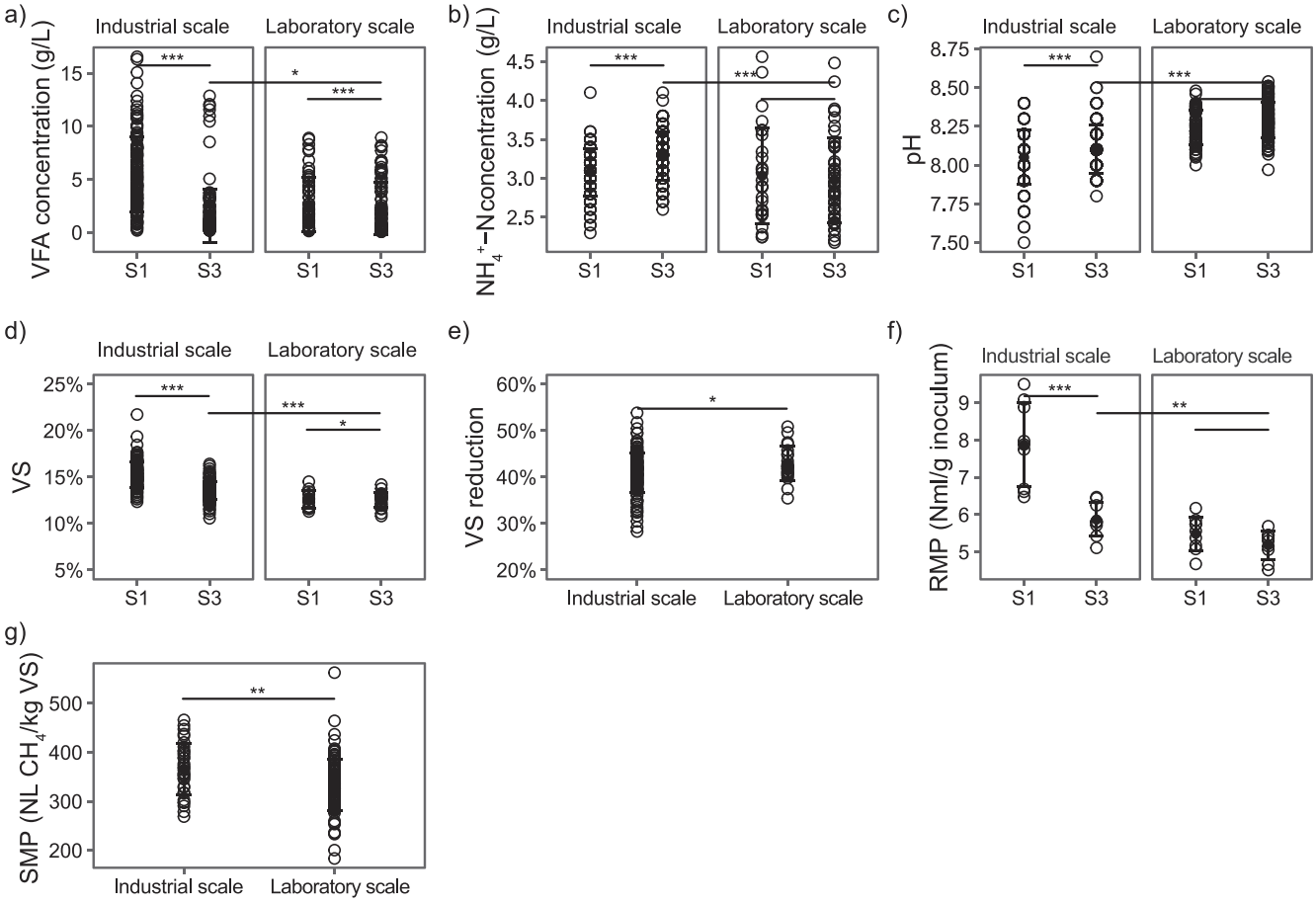

Fig. 3. Process parameters a) total VFA concentration, b) NH_4^+-N concentration, c) pH and d) VS, in industrial-scale and laboratory-scale reactors, with comparison between sections S1 and S3. e) VS-reduction in digestate from S3 relative to substrate VS content (22-23 %). f) RMP in digestate from industrial-scale reactor RK3, sections S1 and S3, and laboratory-scale reactors, sections S1 and S3. g) SMP at industrial and laboratory scale. Asterisks indicate significant differences (*$p < 0.05$, **$p < 0.01$, ***$p < 0.001$).

significantly higher at laboratory (43 %) than industrial scale (41 %) (Fig. 3e). RMP, quantifying the remaining gas potential in the digestate, was significantly higher in outgoing digestate from industrial-scale reactors (5.9 NmL/g digestate) compared with laboratory-scale reactors (5.2 NmL/g digestate) (Fig. 3f). Process efficiency, calculated based on HRT, RMP and volumetric methane production, showed similar values at laboratory and industrial scale (92.5 and 93.1 %, respectively).

At both scales, the dry matter fraction in the digestate was dominated by carbohydrates (53–74 % of TS), followed by protein (13–16 % of TS) and fat (2–5 % of TS) (Table 3). The digestate samples from laboratory-scale reactors had similar composition to the substrate mixtures (in terms of percentages of TS), but with a lower fat content and slightly higher protein fraction in digestate samples (Table 3). In all sections of the laboratory-scale reactors, the reduction in comparison with substrate was similar except for carbohydrates which first decreased by 39 % in S1 and then further to 47 % reduction in S3 (Fig. E.1). The most efficient degradation was obtained for raw fat, which decreased by almost 90 % (Fig. E.1). In samples from the industrial-scale reactors, there were no clear differences between digestate samples from sections S1 and S3 (Table 3).

The degradation rate of different components of the substrate was evaluated by determination of gas production from fat, protein and cellulose in digestate from the different reactor sections (S1 compared with S3). The batch tests with digestate from the laboratory-scale reactors revealed similar initial cellulose degradation rate in both sections, whereas degradation of protein and fat was faster in S1 than in S3 (Fig. E.2). Digestate samples from the industrial-scale reactor showed large variations between replicates in the batch tests and therefore no significant differences between sections could be observed (Fig. E.2).

3.4. Microbial community structure

3.4.1. Community during steady-state

Analyses of microbial community structure using 16S rRNA gene sequencing were performed during a period of stable process operation, with the aim of evaluating differences between laboratory- and industrial-scale reactors, and between sections within reactors. All processes were found to be dominated by *Defluviitoga* (phylum Thermotogota), which accounted for 32–39 % in industrial-scale and 10–14 % in laboratory-scale reactors, and the Clostridia group MBA03 (phylum Bacillota), which accounted for 19–26 % at both laboratory and industrial scale when the process was stable. Other genera with high relative abundance were *Halocella* (phylum Halanaerobiaeota), with relative abundance 6–7 % at laboratory scale and 2–5 % at industrial scale, *Lentimicrobium* (phylum Bacteroidota), with relative abundance 10–11 % and 2–3 % at laboratory and industrial scale, respectively, and the group DTU014 within class Incertae Sedis (phylum Bacillota), which accounted for ~ 7 % of the community at laboratory scale and 3–4 % at industrial scale. Within Archaea, the results demonstrated dominance of genus *Methanothermobacter* within the order Methanobacteriales (phylum Euryarchaeota), accounting for ~ 1 % and 3–10 % of the total community at laboratory and industrial scale, respectively. Another dominant methanogen was *Methanoculleus* within the order Methanomicrobiales (phylum Halobacterota), accounting for 3–6 % and 0–2 % of the total community at laboratory and industrial scale, respectively.

Analysis of β-diversity by weighted PCoA indicated significant differences between industrial and laboratory scale, but no significant differences in community structure between sections (Fig. 4a), sampling time-points or parallel reactors (Fig. F.1). Samples from the inoculum and start-up phase clustered together with the industrial-scale samples (Fig. 4a). Genera that distinctly increased in relative abundance upon downscaling were: *Lentimicrobium* and *Proteiniphilum* from phylum Bacteroidota, *Halocella*, *Acetomicrobium* (phylum Synergistota) and groups within the phylum Bacillota (Firmicutes); Hydrogenispora (order level), DTU014 (order level), *Dethiobacteraceae* (family level) and *Keratinibaculum*. Genera that distinctly decreased in relative abundance upon downscaling were *Defluviitoga* and *Tepidimicrobium* (phylum Bacillota) (Fig. 4b). For Archaea, a shift in the two dominant groups was observed. Higher abundance of *Methanoculleus* in the laboratory-scale reactors and in the inoculum was confirmed by qPCR analysis targeting the two dominant archaeal orders Methanomicrobiales (*i.e. Methanoculleus*) and Methanobacteriales (*i.e. Methanothermobacter*) (Fig. G.1). However, the dominance of Methanobacteriales over Methanomicrobiales in industrial-scale reactors observed in 16S rRNA analysis was not clearly confirmed by qPCR analysis.

3.4.2. Community during process disturbance

To study microbial community dynamics during process disturbances, digestate samples were collected at several time-points during the period of VFA accumulation (Fig. 2e, 2f). These samples were all taken from S3 (*i.e.* no section comparison). In both laboratory-scale reactors (LR1, LR2), there was an increase in relative abundance of *Defluviitoga* and decrease in relative abundance of MBA03 during the disturbance phase, and in LR1 this change was associated with the increase in VFA concentration (Fig. 5a). At the point when VFA concentration decreased in LR1 (around week 45), microbial community structure returned to the original proportions. Industrial-scale reactor RK1 also showed a decrease in relative abundance of MBA03 during the disturbance period, together with a peak in relative abundance of *Methanothermobacter* (Fig. 5b). In both laboratory-scale reactors and in RK1, the genera *Halocella*, *Keratinibaculum* and *Tepidimicrobium* increased in relative abundance simultaneously with the highest VFA concentrations, while there was a decrease in *Lentimicrobium* at the same time-points (Fig. 5a, 5b).

Table 3
Concentrations of raw protein, carbohydrates and raw fat in laboratory-scale substrate mixture and in digestate samples from laboratory- and industrial-scale reactors.

		Lab-scale			Industrial-scale	
Macromolecule	Substrate[b]	S1[c]	S2[c]	S3[d]	S1[c]	S3[c]
TS[a] [%]	25	16	16	16	22	19
Raw protein [% of TS]	11	13	13	13 (1)	14	16
Carbohydrates [% of TS]	60	60	61	53 (5)	71	74
Raw fat [% of TS]	8	2	3	3 (0)	4	5

[a] Mean values over the experiment period.
[b] Mean of two substrate mixes used in laboratory-scale reactors, from week 14–25 and week 26–53, respectively.
[c] Mean for reactors LR1 and LR2 at laboratory scale and for reactors RK2 and RK3 at industrial scale (from one time-point each).
[d] Mean values from reactors LR1 and LR2 from two sampling time-points, standard deviation in brackets.

4. Discussion

4.1. Process performance, downscaling effects and link to the microbial community in laboratory- and industrial-scale reactors

4.1.1. Methane production and substrate degradation in laboratory- and industrial-scale reactors

During the experimental period, mean SMP in the laboratory- and industrial-scale reactors was 338 and 366 NL CH_4/kg VS respectively, which is within the range reported previously for thermophilic co-digestion of food waste (~50 % of VS) and vegetable, straw or garden waste (330–520 NL CH_4/kg VS) [13,14,49,50]. The values obtained were also within the wide range of SMP values (160–420 NL CH_4/kg VS) reported in previous studies of thermophilic high-solid digestion systems treating food waste (80–100 % of VS) [15,32,51]. The differences between studies are likely caused by large differences in operating parameters, such as substrate characteristics, OLR and HRT. The overall VS-reduction was similar in industrial- and laboratory-scale reactors

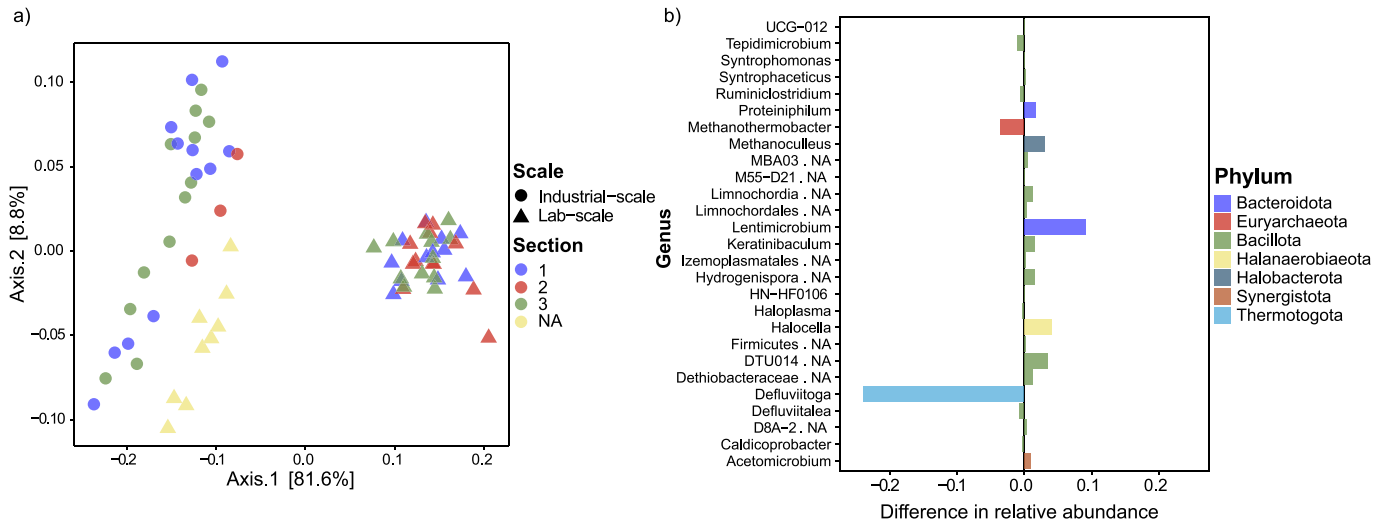

Fig. 4. a) Weighted PCoA plot, with colours indicating samples from different reactor sections at laboratory and industrial scale. Yellow triangles (reactor section not applicable) indicate inoculum and samples from the start-up phase at laboratory scale. Blue, red and green symbols indicate sections S1, S2 and S3, respectively. b) Difference in relative abundance of bacteria and archaea at genus level (colours indicate phyla) in laboratory-scale compared to industrial-scale reactors. Average relative abundances over replicates, time-points, sections and reactors. (For interpretation of the references to colour in this figure legend, the reader is referred to the web version of this article.)

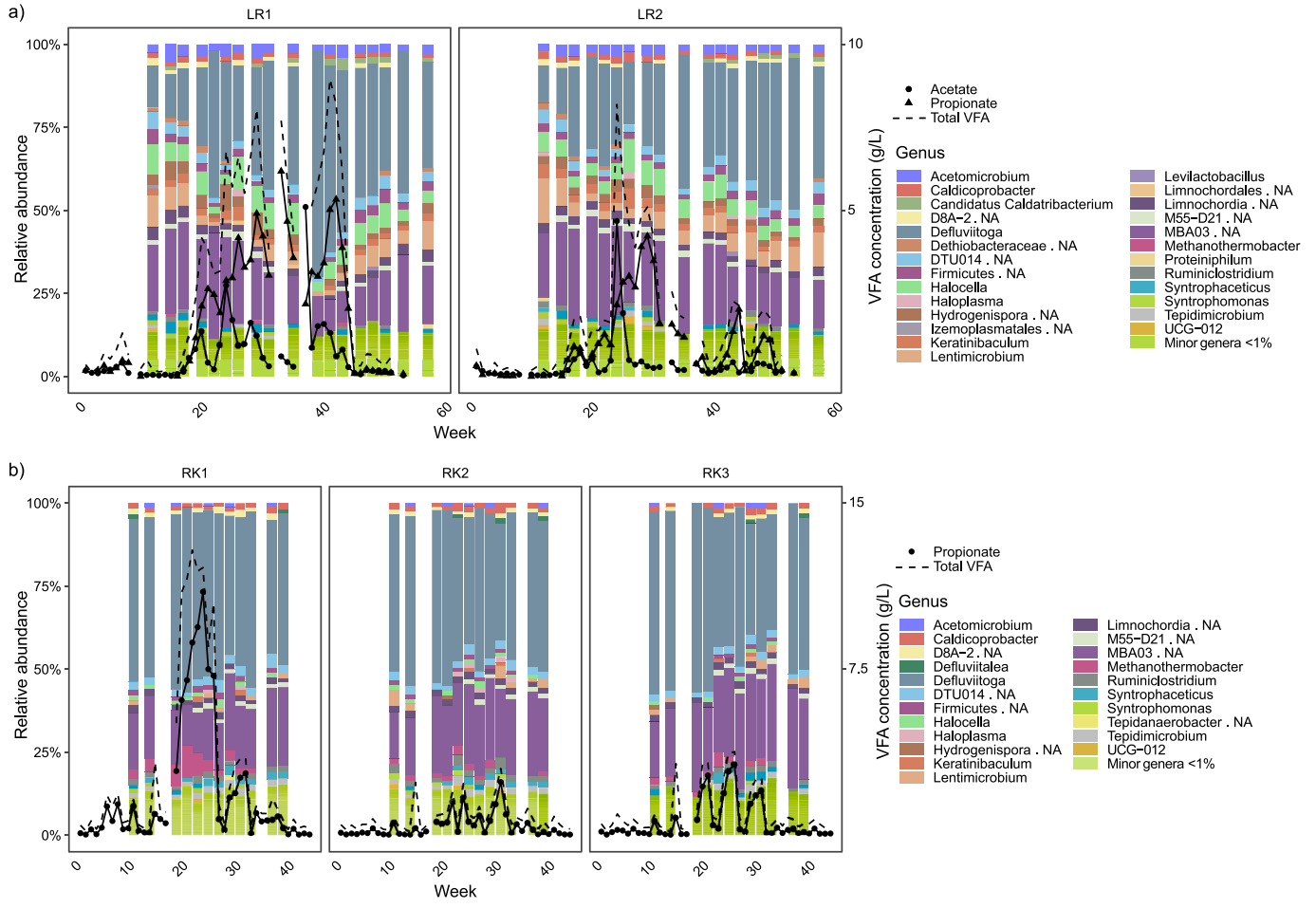

Fig. 5. Relative abundance of bacteria and archaea at genus level in a) laboratory-scale reactors LR1 and LR2, where total VFA concentration in the reactors is indicated by dashed line, acetate and propionate concentrations by circles and triangles, respectively, and b) industrial-scale reactors RK1, RK2 and RK3, where total VFA concentration in the reactors is indicated by dashed line and propionate concentration by circles.

(41–43 %), but at the lower end of the range reported for thermophilic HSD processes digesting food waste (40–70 %) [8,12,15,32]. This result could be expected since the substrate mix used in this study contained only around 50 % food waste and the additional fractions consisted of more recalcitrant lignocellulosic material (*i.e.* horse manure, garden residues and crop residues).

4.1.2. Scale comparison and downscaling effects on overall process efficiency and degree of degradation

When simulating an industrial-scale HSD process at laboratory scale, there are several factors to consider. One is particle size of the substrate and inoculum, which needs to be smaller in a laboratory-scale system. In the present study, the inoculum used for the laboratory-scale reactors was sieved and the substrate was grinded, while rougher shredding and sieving of the substrate was applied at the industrial-scale plant. In addition, the feeding strategy, *i.e.* semi-continuously every day at industrial scale and once per day, six days per week, at laboratory scale, differed for practical reasons. Another difference was substrate composition, which was more consistent in the laboratory and only represented a few samples of the industrial-scale substrate mix. Furthermore, average OLR and HRT differed between the scales. These parameters were initially set according to the operating conditions at the industrial-scale plant, but during the time of the experiment, parameters were changed slightly at the plant.

Despite the above-mentioned differences, process performance was relatively similar at laboratory and industrial scale (Fig. 3). Additionally, overall process efficiency estimated based on volumetric methane production, HRT and RMP [48] was similar for laboratory- and industrial-scale reactors (93 %). However, some small differences were observed, such as slightly higher VS-reduction at laboratory scale (Fig. 3e). This difference could be a result of the additional substrate pretreatment at laboratory scale, potentially increasing substrate availability to microorganisms, and consequently biodegradability and methane production [5,52]. Higher degree of substrate degradation in laboratory-scale reactors was also supported by lower RMP compared with industrial-scale reactors. Additionally, the concentrations of macromolecules (% of TS) in digestate samples were generally slightly higher in industrial-scale (Table 3). Interestingly, in contrast to VS-reduction, SMP was higher (8 %) at industrial scale. Both VS-reduction and RMP pointed towards a higher degree of degradation in laboratory-scale reactors, but the higher level of NH_4^+-N in outgoing digestate from industrial-scale reactors (Fig. 3b, 3e and 3f) instead indicated more efficient protein degradation at the larger scale. However, this difference could also have been caused by greater variability and, on average, higher protein content in the substrate mix at industrial scale. Since proteins in general have higher biomethane potential than *e.g.* lignocellulosic substrates [53], this could potentially explain the higher SMP in the industrial-scale reactors. The larger weekly fluctuations in gas production at laboratory compared with industrial scale (Fig. 2a-b) could also have influenced mean SMP at laboratory scale in a negative way. A similar observation was made in a laboratory-/industrial-scale comparison by Lüdtke *et al.* [35], who speculated that smaller fluctuations in industrial-scale reactors could be a result of more accurate automated feeding and measurement procedures compared with manual operation at laboratory scale. In addition, gas production in industrial-scale reactors in the present study was calculated as a mean value for all three reactors, providing seemingly more stable results compared to separate measurements of gas production from each reactor, which was the procedure in laboratory-scale. Another factor that could have affected average methane production was process disturbances, which were more severe at laboratory scale and only arose in one of the three industrial-scale reactors, which might have lowered average SMP at laboratory scale in comparison with the industrial-scale process.

4.1.3. Microbial community structure in laboratory- and industrial-scale reactors and downscaling effects

In line with previous studies on CSTR reactors [47,54], a downscaling effect was observed on comparing microbial community structure in the laboratory- and industrial-scale processes (Fig. 4a). One cause of this difference may be the different feeding regimes, as previous findings have indicated that feeding frequency has a significant effect on microbial community structure [55]. However, differences in parameters such as OLR, pH, VFA and temperature could also have had an impact (Table 2). Nevertheless, the laboratory- and industrial-scale communities shared strong similarities, *e.g.* dominance of the bacterial group MBA03 and genus *Defluviitoga*. Both these groups have previously been shown to be highly abundant in dry thermophilic AD processes [13,15,56]. The function of MBA03 is not yet known, although it has been suggested to be linked to syntrophic acetate oxidation (SAO) [57] or involved in carbohydrate fermentation [56], while *Defluviitoga* is suggested to be very important for hydrolysis of complex carbohydrates in thermophilic processes [13,56,58]. Another highly abundant genus was *Halocella* which, like *Defluviitoga*, is cellulose-degrading and halophilic [59] and previously has been observed in dry thermophilic digestion processes [15,60]. Another highly abundant genus was *Lentimicrobium*, which is proposed to be involved in acidogenesis in the AD process [61], with the type species growing on starch and simple sugars [62]. However, members of this genus have also been enriched in both acetate- and propionate-fed reactors, and may be involved in acetate degradation [57,63].

Analysis of the carbohydrate-hydrolysing microbial groups upon downscaling revealed a clear decrease in relative abundance of *Defluviitoga*, whereas *Halocella* generally had higher relative abundance in the laboratory-scale than the industrial-scale reactors. Other notable changes were increases in the relative abundance of two genera belonging to phylum Bacteroidota (*Lentimicrobium* and *Proteiniphilum*). In the reactor communities, mainly three genera known to possess proteolytic abilities (*Proteiniphilum* [64], *Keratinibaculum* [65] and the closely related *Tepidimicrobium* [66]) were identified. The relative abundance of *Proteiniphilum* and *Keratinibaculum* increased upon downscaling, while that of *Tepidimicrobium* decreased. These changes in the microbial community indicated shifts in both the proteolytic and saccharolytic groups at laboratory scale compared with the industrial-scale process, but these shifts did not seem to affect the degree of degradation of the corresponding substrates.

For the predominant methanogenic genera, there was a clear shift in dominance by *Methanothermobacter* at industrial scale towards *Methanoculleus* at laboratory scale. Species belonging to *Methanothermobacter* have a growth optimum at 55–65 °C [67], so the slightly higher average temperature in the industrial-scale systems may have favoured growth of this genus. The reason for the increase in *Methanoculleus* relative to *Methanothermobacter* upon downscaling in the present study (Fig. G.1) is not clear, but could be related to the generally lower H_2 level in laboratory-scale than industrial-scale reactors (Fig. B.1). Previous findings suggest that *Methanoculleus* is enriched and has competitive advantage at low levels of H_2 [68,69]. However, no firm conclusions can be drawn on whether the downscaling effect on the methanogenic community influenced overall methane production efficiency.

4.2. Ammonia and VFA levels coupled to microbiology under stable conditions and process disturbance

4.2.1. VFA accumulation in response to high levels of NH_4^+-N

During the entire experimental period, both the laboratory- and industrial-scale processes had high NH_4^+-N levels which, combined with thermophilic conditions and relatively high pH, led to high ammonia concentrations (0.6–2.0 g NH_3-N/L), exceeding levels previously reported to inhibit microorganisms, cause VFA accumulation and decrease methane production in thermophilic systems (0.6–1.5 g NH_3-N/L) [18,70]. In line with this, both laboratory-scale reactors (LR1, LR2) and

one industrial-scale reactor (RK1) showed rapid accumulation of VFA, particularly propionate, when the NH_4^+-N level increased slightly and reached 4.2–4.5 g/L (1.6–2.0 g NH_3-N/L) and 4.1 g/L (0.8 g NH_3-N/L) respectively (Fig. 2g-h, Fig. B.1, Fig. B.2). In laboratory-scale reactors, the increase in NH_3-N was observed after introducing the second batch of substrate mix, which had a relatively high content of fat and protein (Table 1), indicating that the overall high ammonia level made the reactors sensitive to small changes in substrate composition. More severe disturbance and maintained higher propionate concentration were observed in LR1 compared with LR2. This process imbalance could have been caused by technical issues in LR1, such as difficulty maintaining reactor volume and thereby sporadic substrate overloading, in addition to the substrate composition change. Previous studies of thermophilic HSD operating with food waste have also observed signs of disturbance, *e.g.* high propionate levels relative to acetate, upon an increase in OLR [32,71], and in processes with 1.2–1.9 g NH_3-N/L [15]. Accumulation of propionate is considered an important indicator of ammonia inhibition and process disturbance, but also an inhibitor in itself, especially since propionate degradation often has a long lag-phase and elevated levels can persist over a long period [72].

4.2.2. Microbial community structure and links to NH_3-N and process instability

The microbial communities in both laboratory- and industrial-scale reactors were generally dominated by bacterial groups known to be ammonia-tolerant, such as the abundant MBA03 and *Defluviitoga* [15,73]. *Lentimicrobium* has also been observed previously at high NH_4^+-N concentrations in thermophilic conditions [63], as have *Halocella* and DTU014 [15]. Similarly, both dominating methanogenic genera, *Methanothermobacter* and *Methanoculleus,* are known to include members that are ammonia-tolerant. As an example, in bioaugmentation experiments, members of these genera have been shown to significantly improve methane production in ammonia-stressed systems [74,75]. The dominance of these hydrogenotrophic methanogens strongly indicates that, in line with previous findings on thermophilic HSD [15,56,60], the hydrogenotrophic methanogenic pathway was favoured over the acetoclastic in our reactors. Under these conditions, acetate is degraded by syntrophic acetate-oxidising bacteria (SAOB) in cooperation with hydrogenotrophic methanogens [70]. Potential candidate SAOB in the community were MBA03 [57], *Syntrophaceticus* (phylum Bacillota) and *Caldicoprobacter* (phylum Bacillota) [56]. The *Syntrophaceticus* sequence identified in the present study was shown to be identical to the 16S rRNA gene sequence of a novel SAOB candidate that cooperates with *Methanothermobacter* and/or *Methanoculleus* in thermophilic and high-ammonia conditions [76,77]. Also, this genus has previously been shown to comprise a mesophilic SAOB species that cooperates with *Methanoculleus* to degrade acetate [78].

Microbial community structure was studied over time during process disturbance, to reveal the microbial response to high ammonia and VFA levels at both scales. In agreement with Lv *et al.* [79], who observed different changes in community structure in parallel reactors upon ammonia inhibition, all three disturbed reactors (LR1, LR2, RK1) in the present study showed slightly different responses (Fig. 5a-b). Interestingly, after the decrease in relative abundance of *Defluviitoga* upon downscaling, this genus increased again in laboratory-scale reactor LR1 to a peak where it accounted for > 60 % of the total microbial community, which coincided with the NH_4^+-N and VFA peaks. There was also a slow increase in *Defluviitoga* in reactor LR2 during the course of the experiment, but a similar peak in relative abundance was not seen in this reactor. At industrial scale, no difference in relative abundance of *Defluviitoga* was seen between reactors or over time, even in RK1 during the disturbance phase. Thus the link between this genus and reactor instability is not clear. However, the type species, *Defluviitoga tunisiensis*, is known to produce acetate, CO_2 and H_2 [58] and thus the high relative abundance of *Defluviitoga* in LR1 may have contributed to the relatively high acetate levels in that reactor.

Interestingly, in contrast to the laboratory-reactors, the degradation of propionate in RK1 was relatively rapid, which was possibly explained by the lower level of free ammonia in industrial-scale compared with laboratory-scale reactors (Fig. 2e-h, Table 2). An alternative explanation could be the pronounced change in relative abundance of *Methanothermobacter* in reactor RK1, which peaked at > 9 % of the total community during the disturbance period. Singh *et al.* [77] observed that efficient propionate degradation at thermophilic temperature is strongly linked to activity of *Methanothermobacter*. Thus, the high levels of this methanogen in industrial-scale compared with laboratory-scale reactors suggests that *Methanothermobacter* could have played a role in achieving efficient propionate oxidation in the former. A similar pronounced change in relative abundance of methanogens was not observed at laboratory scale. Looking specifically at possible propionate-degrading bacteria, sequences here assigned to *Pelotomaculum* were found to be identical to the potential thermophilic and ammonia-tolerant syntrophic propionate-oxidising bacteria '*Candidatus* Thermosyntrophopropionicum ammoniitolerans' [77]. That species showed low relative abundance (<0.2 %) at all time-points but could still have contributed to propionate degradation, as syntrophic VFA degraders can be present in very low abundance but still be essential for a stable process [80]. Similarly, the potential syntrophic acetate oxidisers *Syntrophaceticus* and *Caldicoprobacter* increased only slightly in relative abundance as a response to peaks in acetate concentration in the laboratory-scale reactors. Relative abundance of MBA03 instead declined during the VFA and ammonia peak, but it was still one of the dominant groups in all reactors. Thus, no clear correlation between VFA level and the relative abundance of potential VFA oxidising groups could be observed.

4.3. Evaluation of plug-flow behaviour and phase separation

The occurrence of phase separation or plug-flow behaviour in laboratory-scale reactors of plug-flow type has been investigated in some previous studies. For instance, Rossi *et al.* [32] studied microbial communities and VFA production in different sections of a thermophilic laboratory-scale plug-flow reactor digesting organic household waste. Plug-flow was also confirmed by Nordell *et al.* [30] in a tracer test in a laboratory-scale reactor operating with dewatered digestate of sewage sludge. Here, the industrial-scale reactors showed indications of phase separation across the reactor, with higher VFA concentration and VS in the first section and higher pH and NH_4^+-N concentration in the outgoing digestate (Fig. 3a-d, Table C.1). If the PFR is assumed to work as a serial digester system, the first step is expected to have a higher hydrolysis and acidification activity, which would lead to higher VFA levels and lower pH [47,81]. In contrast, the last step of a serial system is expected to have more complete degradation and thereby lower VS and VFA levels, but also accumulation of NH_4^+-N [47,82]. However, in the laboratory-scale system of the present study, the levels of NH_4^+-N, pH, VFA, and VS were relatively similar in different sections (Fig. 3a-d, Table C.1), indicating absence of phase-separation, and the behaviour was instead more similar to a single CSTR. The slight phase separation observed in industrial-scale reactors could be a sign of plug-flow behaviour but could possibly also be explained by the sampling and feeding strategy. In laboratory-scale reactors, samples were always taken a day after the previous feeding, while in industrial-scale reactors, samples were taken during continuous feeding, when theoretically *e.g.* the VFA levels are higher [55,83]. Also, this means that samples taken in the first section in the industrial-scale process most likely included some newly fed substrate, which could have contributed to the higher VS level in this section.

At laboratory scale, some differences were still observed between the reactor sections, *e.g.* slightly faster protein and fat degradation in S1 compared with S3 (Fig. E.2). Furthermore, lower carbohydrate concentration towards the end of the laboratory-scale reactors (Table 3, Fig. E.1) indicated slightly better degree of degradation in the last

section. Unfortunately, it could not be confirmed whether the same trends were obtained in the industrial scale reactors since the results from the batch tests showed high variation between replicates (Fig. E.2), probably due to the inhomogenous nature of the digestate samples from the larger scale reactors. Also, there were no clear differences in macromolecule concentrations between S1 and S3 in industrial scale (Table 3). Based on microbial community structure and the results of PCoA analysis (Fig. 4a), there was no significant difference between the sections in either laboratory- or industrial-scale reactors. It is routine practice at the industrial-scale plant to reinoculate the first section of the plug-flow reactor with digestate, which has been observed to increase process stability [30]. Such recirculation of digestate might have contributed to homogenize the microbial community across the sections, potentially hindering separation of the AD steps in the reactor. However, Rossi *et al.* [32] observed significantly different microbial communities in different sections of a laboratory-scale plug-flow reactor, with higher relative abundances of *Defluviitoga* in the first and last section, and higher relative abundance of protein-degrading genera in the middle. This was achieved using a digestate recirculation ratio of 45 %, indicating that recirculation alone does not explain the lack of phase separation. In line with this, Chen *et al.* [31] obtained a significantly different microbial community at the inlet of a plug-flow reactor than in the middle and last sections, even with recirculation ratio as high as 50–60 %. There are several factors that potentially contributed to better phase separation in those studies, such as substrate characteristics, different recirculation ratios and mixer properties. Another important factor in reactor design is length:width (L:W) ratio, which was 4.1 in our laboratory-scale reactors (5.3 in the industrial-scale reactors), while in other studies using laboratory-scale plug-flow type reactors it has typically been slightly higher, *e.g.* 4.4 [84], 6 [30], 10.8 [85], 12 [31], 15.7 [86] or 30 [87]. Unfortunately, of the above mentioned studies, only Nordell *et al.* [30] and Chen *et al.* [31] investigated plug-flow behaviour or phase separation, which makes it difficult to draw conclusions about which conditions are key factors for obtaining a plug-flow. Phase separation can be achieved, and short-circuiting reduced, if the PFR is compartmentalised or the design in some way hinders material from flowing freely through the reactor [87–89]. More research is needed to fully understand the extent to which this can affect yield and process efficiency.

The tracer tests carried out both in laboratory- and industrial-scale confirmed that there was no plug-flow behaviour in the reactors. Theoretically, in an ideal plug-flow system the peak in outgoing tracer would come after one HRT, but the Li^+-concentration curve in the laboratory-scale (Fig. D.1 and D.2) instead resembled that of a completely stirred reactor, with the peak in tracer appearing within the first few days after addition [24]. Although the duration of the tracer test in industrial-scale reactors was not long enough to obtain a tracer curve for an entire HRT, the results indicated short-circuiting also in this system and ingoing material started to flow out already within the first 24 h.

5. Conclusions

This comparison of a laboratory- and industrial-scale process highlighted some of the difficulties that can arise in direct comparisons of systems at different scales. The main differences were the substrate mix (more non-homogeneous, larger particle size and more varying in industrial- compared with laboratory-scale), digestate characteristics (particle size) and feeding strategy. However, the differences in process parameters, efficiency and yield were relatively small, indicating that the laboratory-scale system represented a good approximation of the industrial-scale system over time.

Within the microbial community, pairs or groups of genera with similar suggested functions in the AD process were identified, where one genus decreased upon downscaling while the other increased. Examples were the saccharolytic genera *Halocella* and *Defluviitoga*, the proteolytic genera *Proteiniphilum*, *Keratinibaculum* and *Tepidimicrobium* and the hydrogenotrophic methanogens *Methanoculleus* and *Methanothermobacter*. Thus these might have replaced each other to adapt to the slightly altered conditions in the laboratory compared with the industrial-scale process, without significant loss of efficiency and productivity by the overall microbial community.

Process disturbances occurred in laboratory- and industrial-scale reactors when the NH_4^+-N level reached > 4 g/L and led to accumulation of VFA, especially propionate. Both processes were run at relatively high NH_4^+-N levels throughout the experimental period, which likely increased the risk of even small changes in *e.g.* substrate composition inducing process disturbance, highlighting the importance of continuous process monitoring. Additionally, a potential link between high relative abundance of *Methanothermobacter* and propionate degradation was observed during the disturbance phase.

The results obtained at both laboratory and industrial scale indicated no plug-flow behaviour, suggesting that high-solid digestion in reactors of plug-flow type is perhaps not utilized to its full potential. Theoretically, a true plug-flow system has several advantages over CSTR processes, such as reduced short-circuiting and the possibility to obtain phase separation. To conclude, more investigation is needed to determine how to operate an HSD process to achive plug-flow and better exploit its potential advantages.

CRediT authorship contribution statement

Ebba Perman: Formal analysis, Investigation, Writing – original draft, Visualization, Project administration. **Maria Westerholm:** Conceptualization, Writing – review & editing, Supervision, Funding acquisition. **Tong Liu:** Supervision. **Anna Schnürer:** Conceptualization, Writing – review & editing, Supervision, Funding acquisition.

Declaration of competing interest

The authors declare that they have no known competing financial interests or personal relationships that could have appeared to influence the work reported in this paper.

Data availability

16S rRNA-gene sequence data can be accessed at BioProject accession numbers PRJNA1011979 and PRJNA1012582 at Sequence Read Archive (SRA), National Center for Biotechnology Information (NCBI).

Acknowledgments

The authors would like to thank Simon Isaksson at the Swedish University of Agricultural Sciences (SLU), Uppsala, Sweden, for laboratory assistance and expertise, and Sara Simon for help with data collection, sampling and substrate collection at the industrial-scale plant. Research Institutes of Sweden (RISE) in Uppsala is acknowledged for help in designing, constructing and maintaining the laboratory-scale reactors. This project was funded by Kamprad Family Foundation (project no. 20200626), SLU and the Biogas Solutions Research Center (BSRC), Linköping, Sweden, which in turn is funded by the Swedish Energy Agency (grant number P2021-90266). The authors declare no conflict of interest.

Appendix A. Supplementary data

Supplementary data to this article can be found online at https://doi.org/10.1016/j.enconman.2023.117978.

References

[1] Anukam A, Mohammadi A, Naqvi M, Granström K. A Review of the Chemistry of Anaerobic Digestion: Methods of Accelerating and Optimizing Process Efficiency. Processes 2019;7(8):504.
[2] Börjesson P, Mattiasson B. Biogas as a resource-efficient vehicle fuel. Trends Biotechnol 2007;26(1):7–13.
[3] Möller K, Müller T. Effects of anaerobic digestion on digestate nutrient availability and crop growth: A review. Eng Life Sci 2012;12(3):242–57.
[4] Baştabak B, Koçar G. A review of the biogas digestate in agricultural framework. J Mater Cycles Waste Manag 2020;22(5):1318–27.
[5] Sarker S, Lamb JJ, Hjelme DR, Lien KM. A Review of the Role of Critical Parameters in the Design and Operation of Biogas Production Plants. Appl Sci 2019;9(9):1915.
[6] André L, Pauss A, Ribeiro T. Solid anaerobic digestion: State-of-art, scientific and technological hurdles. Bioresour Technol 2018;247:1027–37.
[7] Fagbohungbe MO, Dodd IC, Herbert BMJ, Li H, Ricketts L, Semple KT. High solid anaerobic digestion: Operational challenges and possibilities. Environ Technol Innov 2015;4:268–84.
[8] Karthikeyan OP, Visvanathan C. Bio-energy recovery from high-solid organic substrates by dry anaerobic bio-conversion processes: a review. Rev Environ Sci Biotechnol 2013;12(3):257–84.
[9] Kothari R, Pandey KA, Kumar S, Tyagi VV, Tyagi SK. Different aspects of dry anaerobic digestion for bio-energy: An overview. Renew Sust Energ Rev 2014;39:174–95.
[10] Morris BEL, Henneberger R, Huber H, Moissl-Eichinger C. Microbial syntrophy: interaction for the common good. FEMS Microbiol Rev 2013;37:384–406.
[11] Alavi-Borazjani SA, Capela I, Tarelho LAC. Over-acidification control strategies for enhanced biogas production from anaerobic digestion: A review. Biomass Bioenergy 2020;143:105833.
[12] Rocamora I, Wagland ST, Villa R, Simpson EW, Fernández O, Bajón-Fernández Y. Dry anaerobic digestion of organic waste: A review of operational parameters and their impact on process performance. Bioresour Technol 2020;299:122681.
[13] Zhang S, Xiao M, Liang C, Chui C, Wang N, Shi J, et al. Multivariate insights into enhanced biogas production in thermophilic dry anaerobic co-digestion of food waste with kitchen waste or garden waste: Process properties, microbial communities and metagenomic analyses. Bioresour Technol 2022;361:127684.
[14] Zeshan OP, Karthikeyan C. Visvanathan, Effect of C/N ratio and ammonia-N accumulation in a pilot-scale thermophilic dry anaerobic digester. Bioresour Technol 2012;113:294–302.
[15] Westerholm M, Liu T, Schnürer A. Comparative study of industrial-scale high-solid biogas production fromfood waste: Process operation and microbiology. Bioresour Technol 2020;304:122981.
[16] Rocamora I, Wagland ST, Hassard F, Villa R, Peces M, Simpson EW, et al. Inhibitory mechanisms on dry anaerobic digestion: Ammonia, hydrogen and propionic acid relationship. Waste Manage 2023;161:29–42.
[17] Chen Y, Cheng JJ, Creamer KS. Inhibition of anaerobic digestion process: A review. Bioresour Technol 2008;99:4044–64.
[18] Rajagopal R, Massé DI, Singh G. A critical review on inhibition of anaerobic digestion process by excess ammonia. Bioresour Technol 2013;143:632–41.
[19] David A, Govil T, Tripathi A, McGeary J, Farrar K, Sani R. Thermophilic Anaerobic Digestion: Enhanced and Sustainable Methane Production from Co-Digestion of Food and Lignocellulosic Wastes. Energies 2018;11(8):2058.
[20] Perin JKH, Borth PLB, Torrecilhas AR, Santana da Cunha L, Kuroda EK, Fernandes F. Optimization of methane production parameters during anaerobic co-digestion of food waste and garden waste. J Clean Prod 2020;272:123130.
[21] Rossi E, Pecorini I, Ferrara G, Iannelli R. Dry Anaerobic Digestion of the Organic Fraction of Municipal Solid Waste: Biogas Production Optimization by Reducing Ammonia Inhibition. Energies 2022;15(15):5515.
[22] Akinbomi JG, Patinvoh RJ, Taherzadeh MJ. Current challenges of high-solid anaerobic digestion and possible measures for its effective applications: a review. Biotechnol biofuels bioprod 2022;15(1).
[23] Donoso-Bravo A, Sadino-Riquelme C, Gómez D, Segura C, Valdebenito E, Hansen F. Modelling of an anaerobic plug-flow reactor. Process analysis and evaluation approaches with non-ideal mixing considerations. Bioresour Technol 2018;260:95–104.
[24] Toson P, Doshi P, Jajcevic D. Explicit Residence Time Distribution of a Generalised Cascade of Continuous Stirred Tank Reactors for a Description of Short Recirculation Time (Bypassing). Processes 2019;7(9):615.
[25] Roy CS, Talbot G, Topp E, Beaulieu C, Palin M-F, Masse DI. Bacterial community dynamics in an anaerobic plug-flow type bioreactor treating swine manure. Water Res 2009;43(1):21–32.
[26] Liu T, Ghosh S. Phase separation during anaerobic fermentation of solid substrates in an innovative plug-flow reactor. Wat Sci Tech 1997;36:303–10.
[27] Moestedt J, Nordell E, Yekta SS, Lundgren J, Martí M, Sundberg C, et al. Effects of trace element addition on process stability during anaerobic co-digestion of OFMSW and slaughterhouse waste. Waste Manage 2015;47:11–20.
[28] Panaro DB, Mattei MR, Esposito G, Steyer JP, Capone F, Frunzo L. A modelling and simulation study of anaerobic digestion in plug-flow reactors. Commun Nonlinear Sci Numer Simul 2022;105:106062.
[29] Benbelkacem H, Bollon J, Bayard R, Escudié R, Buffière P. Towards optimization of the total solid content in high-solid (dry) municipal solid waste digestion. Chem Eng J 2015;273:261–7.
[30] Nordell E, Moestedt J, Österman J, Yekta SS, Björn A, Sun L, et al. Post-treatment of dewatered digested sewage sludge by thermophilic high-solid digestion for pasteurization with positive energy output. Waste Manage 2021;119:11–21.
[31] Chen R, Li Z, Feng J, Zhao L, Yu J. Effects of digestate recirculation ratios on biogas production and methane yield of continuous dry anaerobic digestion. Bioresour Technol 2020;316:123963.
[32] Rossi E, Becarelli S, Pecorini I, Di Gregorio S, Iannelli R. Anaerobic Digestion of the Organic Fraction of Municipal Solid Waste in Plug-Flow Reactors: Focus on Bacterial Community Metabolic Pathways. Water 2022;14(2):195.
[33] Gallert C, Henning A, Winter J. Scale-up of anaerobic digestion of the biowaste fraction from domestic wastes. Water Res 2003;37:1433–41.
[34] Bouallagui H, Marouani L, Hamdi M. Performances comparison between laboratory and full-scale anaerobic digesters treating a mixture of primary and waste activated sludge. Resour Conserv Recycl 2010;55(1):29–33.
[35] Lüdtke M, Nordberg Å, Baresel C. Experimental power of laboratory-scale results and transferability to full-scale anaerobic digestion. Water Sci Technol 2017;76(4):983–91.
[36] Hansen KH, Angelidaki I, Ahring BK. Anaerobic digestion of swine manure: inhibition by ammonia. Water Res 1998;32:5–12.
[37] Westerholm M, Hansson M, Schnürer A. Improved biogas production from whole stillage by co-digestion with cattle manure Bioresour. Technol 2012;114:314–9.
[38] Anderson GK, Campos CMM, Chernicharo CAL, Smith LC. Evaluation of the inhibitory effects of lithium when used as a tracer for anaerobic digesters. Wat Res 1991;25:755–60.
[39] Danielsson R, Dicksved J, Sun L, Gonda H, Müller B, Schnürer A, et al. Methane Production in Dairy Cows Correlates with Rumen Methanogenic and Bacterial Community Structure. Front Microbiol 2017;8.
[40] Callahan BJ, McMurdie PJ, Rosen MJ, Han AW, Johnson AJA, Holmes SP. DADA2: High-resolution sample inference from Illumina amplicon data. Nat Methods 2016;13(7):581–3.
[41] Weinstein MM, Prem A, Jin M, Tang S, Bhasin JM, Figaro,. An efficient and objective tool for optimizing microbiome rRNA gene trimming parameters. Cold Spring Harbor Laboratory; 2019.
[42] C. Quast, E. Pruesse, P. Yilmaz, J. Gerken, T. Schweer, P. Yarza, J. Peplies, F.O. Glöckner, The SILVA ribosomal RNA gene database project: improved data processing and web-based tools, Nucleic Acids Res. 41 (2013) D590-D596.
[43] Lozupone C, Knight R. UniFrac: a New Phylogenetic Method for Comparing Microbial Communities. Appl Environ Microbiol 2005;71(12):8228–35.
[44] Saitou N, Nei M. The neighbor-joining method: a new method for reconstructing phylogenetic trees. Mol Biol Evol 1987;4:406–25.
[45] Yu Y, Lee C, Kim J, Hwang S. Group specific primer and probe sets to detect methanogenic communities using quantitative real-time polymerase chain reaction. Biotechnol Bioeng 2005;89:670–9.
[46] Ahlberg-Eliasson K, Westerholm M, Isaksson S, Schnürer A. Anaerobic Digestion of Animal Manure and Influence of Organic Loading Rate and Temperature on Process Performance, Microbiology, and Methane Emission From Digestates. Front Energy Res 2021;9:740314.
[47] Perman E, Schnürer A, Björn A, Moestedt J. Serial anaerobic digestion improves protein degradation and biogas production from mixed food waste. Biomass Bioenergy 2022;161:106478.
[48] Rico C, Muñoz N, Rico JL. Anaerobic co-digestion of cheese whey and the screened liquid fraction of dairy manure in a single continuously stirred tank reactor process: Limits in co-substrate ratios and organic loading rate. Bioresour Technol 2015;189:327–33.
[49] Zhang L, Kuroki A, Loh K-C, Seok JK, Dai Y, Tong YW. Highly efficient anaerobic co-digestion of food waste and horticultural waste using a three-stage thermophilic bioreactor: Performance evaluation, microbial community analysis, and energy balance assessment. Energy Convers Manag 2020;223:113290.
[50] Shi X, Guo X, Zuo J, Wang Y, Zhang M. A comparative study of thermophilic and mesophilic anaerobic co-digestion of food waste and wheat straw: Process stability and microbial community structure shifts. Waste Manage 2018;75:261–9.
[51] Bolzonella D, Innocenti L, Pavan P, Traverso P, Cecchi F. Semi-dry thermophilic anaerobic digestion of the organic fraction of municipal solid waste: focusing on the start-up phase. Bioresour Technol 2003;86:123–9.
[52] Müller JA. Comminution of Organic Material. Chem Eng Technol 2003;26(2):207–17.
[53] Li Y, Zhang R, Liu G, Chen C, He Y, Liu X. Comparison of methane production potential, biodegradability, and kinetics of different organic substrates. Bioresour Technol 2013;149:565–9.
[54] Westerholm M, Castillo MDP, Chan Andersson A, Jahre Nilsen P, Schnurer A. Effects of thermal hydrolytic pre-treatment on biogas process efficiency and microbial community structure in industrial- and laboratory-scale digesters. Waste Manage 2019;95:150–60.
[55] Mulat DG, Jacobi HF, Feilberg A, Adamsen APS, Richnow H-H, Nikolausz M. Changing Feeding Regimes To Demonstrate Flexible Biogas Production: Effects on Process Performance, Microbial Community Structure, and Methanogenesis Pathways. Appl Environ Microbiol 2016;82(2):438–49.
[56] Dyksma S, Jansen L, Gallert C. Syntrophic acetate oxidation replaces acetoclastic methanogenesis during thermophilic digestion of biowaste. Microbiome 2020;8(1).
[57] Zheng D, Wang H, Gou M, Nubo MK, Narihiro T, Hu B, et al. Identification of novel potential acetate-oxidizing bacteria in thermophilic methanogenic chemostats by DNA stable isotope probing. Appl Microbiol Biotechnol 2019;103:8631–45.
[58] Ben Hania W, Godbane R, Postec A, Hamdi M, Ollivier B, Fardeau M-L. *Defluviitoga tunisiensis* gen. nov., sp nov., a thermophilic bacterium isolated from a mesothermic and anaerobic whey digester. Int J Syst Evol Microbiol 2012;62:1377–82.
[59] Simankova MV, Chernych NA, Osipov GA, Zavarzin GA. *Halocella cellulolytica* gen. nov., sp. nov., a new obligately anaerobic, halophilic, cellulolytic bacterium. Syst Appl Microbiol 1993;16(3):385–9.

[60] Tang Y-Q, Ji P, Hayashi J, Koike Y, Wu X-L, Kida K. Characteristic microbial community of a dry thermophilic methanogenic digester: its long-term stability and change with feeding. Appl Microbiol Biotechnol 2011;91(5):1447–61.
[61] Wang Y, Wei W, Huang Q-S, Ni B-J. Methane production from algae in anaerobic digestion: Role of corncob ash supplementation. J Clean Prod 2021;327:129485.
[62] Sun L, Toyonaga M, Ohashi A, Tourlousse DM, Matsuura N, Meng X-Y, et al. Lentimicrobium saccharophilum gen. nov., sp. nov., a strictly anaerobic bacterium representing a new family in the phylum Bacteroidetes, and proposal of Lentimicrobiaceae fam. nov. Int J Syst Evol Microbiol 2016;66(7):2635–42.
[63] Li M-T, Rao L, Wang L, Gou M, Sun Z-Y, Xia Z-Y, et al. Bioaugmentation with syntrophic volatile fatty acids-oxidizing consortia to alleviate the ammonia inhibition in continuously anaerobic digestion of municipal sludge. Chemosphere 2022;288:132389.
[64] Chen S, Dong X. *Proteiniphilum acetatigenes* gen. nov., sp. nov., from a UASB reactor treating brewery wastewater. Int J Syst Evol Microbiol 2005;55:2257–61.
[65] Huang Y, Sun Y, Ma S, Chen L, Zhang H, Deng Y. Isolation and characterization of Keratinibaculum paraultunense gen. nov., sp. nov., a novel thermophilic, anaerobic bacterium with keratinolytic activity. FEMS Microbiol Lett 2013;345(1):56–63.
[66] Slobodkin AI, Tourova TP, Kostrikina NA, Lysenko AM, German KE, Bonch-Osmolovskaya EA, et al. Tepidimicrobium ferriphilum gen. nov., sp. nov., a novel moderately thermophilic, Fe(III)-reducing bacterium of the order Clostridiales. Int J Syst Evol Microbiol 2006;56(2):369–72.
[67] Wasserfallen A, Nölling J, Pfister P, Reeve J, Conway de Macario E. Phylogenetic analysis of 18 thermophilic Methanobacterium isolates supports the proposals to create a new genus, Methanothermobacter gen. nov., and to reclassify several isolates in three species, Methanothermobacter thermautotrophicus comb. nov., Methanothermobacter wolfeii comb. nov., and Methanothermobacter marburgensis sp. nov. Int J Syst Evol Microbiol 2000;50:43–53.
[68] Neubeck A, Sjöberg S, Price A, Callac N, Schnürer A. Effect of nickel levels on hydrogen partial pressure and methane production in methanogens. PLoS One 2016;11:e0168357.
[69] Kato S, Takashino M, Igarashi K, Mochimaru H, Mayumi D, Tamaki H. An iron corrosion-assisted H2-supplying system: a culture method for methanogens and acetogens under low H2 pressures. Sci Rep 2020;10(1).
[70] Westerholm M, Moestedt J, Schnurer A. Biogas production through syntrophic acetate oxidation and deliberate operating strategies for improved digester performance. Appl Energy 2016;179:124–35.
[71] Rossi E, Pecorini I, Paoli P, Iannelli R. Plug-flow reactor for volatile fatty acid production from the organic fraction of municipal solid waste: Influence of organic loading rate. J Environ Chem Eng 2022;10(1):106963.
[72] Westerholm M, Calusinska M, Dolfing J. Syntrophic propionate-oxidizing bacteria in methanogenic systems. FEMS Microbiol Rev 2021;46:1–26.
[73] Calusinska M, Goux X, Fossepre M, Muller EEL, Wilmes P, Delfosse P. A year of monitoring 20 mesophilic full-scale bioreactors reveals the existence of stable but different core microbiomes in bio-waste and wastewater anaerobic digestion systems. Biotechnol Biofuels 2018;11.
[74] Yan M, Treu L, Campanaro S, Tian H, Zhu X, Khoshnevisan B, et al. Effect of ammonia on anaerobic digestion of municipal solid waste: Inhibitory performance, bioaugmentation and microbiome functional reconstruction. Chem Eng J 2020;401:126159.
[75] Yan M, Zhu X, Treu L, Ravenni G, Campanaro S, Goonesekera EM, et al. Comprehensive evaluation of different strategies to recover methanogenic performance in ammonia-stressed reactors. Bioresour Technol 2021;336:125329.
[76] Westerholm M, Müller B, Singh A, Karlsson Lindsjö O, Schnürer A. Detection of novel syntrophic acetate-oxidising bacteria from biogas processes by continuous acetate enrichment approaches. Microb Biotechnol 2018;11:680–93.
[77] Singh A, Schnürer A, Dolfing J, Westerholm M. Syntrophic entanglements for propionate and acetate oxidation under thermophilic and high-ammonia conditions. ISME J 2023.
[78] Westerholm M, Roos S, Schnürer A. *Syntrophaceticus schinkii* gen. nov., sp. nov., an anaerobic, syntrophic acetate-oxidizing bacterium isolated from a mesophilic anaerobic filter. FEMS Microbiol Lett 2010;309:100–4.
[79] Lv Z, Leite AF, Harms H, Glaser K, Liebetrau J, Kleinsteuber S, et al. Microbial community shifts in biogas reactors upon complete or partial ammonia inhibition. Appl Microbiol Biotechnol 2019.
[80] Fujimoto M, Carey DE, Zitomer DH, McNamara PJ. Syntroph diversity and abundance in anaerobic digestion revealed through a comparative core microbiome approach. Appl Microbiol Biotechnol 2019;103:6353–67.
[81] Moestedt J, Nordell E, Hallin S, Schnürer A. Two-stage anaerobic digestion for reduced hydrogen sulphide production. J Chem Technol Biotechnol 2016;91(4):1055–62.
[82] Wen Z, Frear C, Chen S. Anaerobic digestion of liquid dairy manure using a sequential continuous-stirred tank reactor system. J Chem Technol Biotechnol 2007;82(8):758–66.
[83] Maurus K, Kremmeter N, Ahmed S, Kazda M. High-resolution monitoring of VFA dynamics reveals process failure and exponential decrease of biogas production. Biorefin: Biomass Convers; 2021.
[84] Gómez, S. Ramos, Fernández, Muñoz, Tey, G. Romero, Hansen, Development of a Modified Plug-Flow Anaerobic Digester for Biogas Production from Animal Manures, Energies 12(13) (2019) 2628.
[85] Eftaxias A, Georgiou D, Diamantis V, Aivasidis A. Performance of an anaerobic plug-flow reactor treating agro-industrial wastes supplemented with lipids at high organic loading rate. Waste Manag Res 2021;39(3):508–15.
[86] Patinvoh RJ, Kalantar Mehrjerdi A, Sárvári Horváth I, Taherzadeh MJ. Dry fermentation of manure with straw in continuous plug flow reactor: Reactor development and process stability at different loading rates. Bioresour Technol 2017;224:197–205.
[87] Dong LL, Cao GL, Wu JW, Yang SS, Ren NQ. Reflux of acidizing fluid for enhancing biomethane production from cattle manure in plug flow reactor. Bioresour Technol 2019;284:248–55.
[88] Massé DI, Gilbert Y, Saady NMC, Liu C. Low-temperature anaerobic digestion of swine manure in a plug-flow reactor. Environ Technol 2013;34(18):2617–24.
[89] Namsree P, Suvajittanont W, Puttanlek C, Uttapap D, Rungsardthong V. Anaerobic digestion of pineapple pulp and peel in a plug-flow reactor. J Environ Manage 2012;110:40–7.